GPS Receiver Architecture and Expected Performance for Autonomous GPS Navigation in Highly Eccentric Orbits

Michael Moreau, Penina Axelrad
Colorado Center for Astrodynamics Research, University of Colorado at Boulder

James L. Garrison
NASA Goddard Space Flight Center

David Kelbel, Anne Long
Computer Sciences Corporation

ABSTRACT

A growing number of science missions call for autonomous spacecraft navigation or formation flying capabilities in highly eccentric orbits (HEO). A study of GPS receiver architectures designed to enable the application of GPS to these types of missions is presented. These HEO receiver architectures are based upon the Goddard Space Flight Center's (GSFC) PiVoT receiver hardware. It features a robust navigation filter coupled with customizations to the satellite selection and acquisition algorithms, and improvements to the tracking loop design to enable improved tracking of weak GPS signals. Several weak signal tracking techniques appearing in the literature are potentially applicable to reduce the tracking threshold and to improve GPS signal visibility in HEO applications. The performance improvement achieved by weak signal tracking is simulated for several characteristic HEO missions. The GPS signal visibility and navigation solution accuracy are compared considering different assumed values for the tracking threshold of the receiver. For a scenario exhibiting very poor GPS visibility, modest reductions in receiver tracking threshold of only 5 to 7 dB are shown to result in a 50 to 60 percent reduction in root-mean-square (RMS) navigation position and velocity errors.

INTRODUCTION

The prospect of using GPS for autonomous navigation of satellites in HEO and geosynchronous (GEO) orbits has been considered for some time with the goal of increasing spacecraft autonomy and reducing system operations costs. Recently, researchers have started developing satellite missions in HEO that require onboard orbit information for formation flying and coordination of multiple spacecraft (Table 1). This paper summarizes the requirements for a GPS receiver to serve in this capacity and outlines some recommended approaches to enhance receiver performance and their expected impact on navigation accuracy in HEO.

Table 1: HEO Communications and Scientific Missions Proposed or Under Development

Mission	Orbit Altitudes	Notes
AMSAT Phase 3D[1]	4000 x 42,000 km	Comm. satellite Launch TBD
Ellipso[2]	8050 km circular 633 x 7605 km sun-synchronous	Constellation of 15 comm. satellites First launch: 1999
IMAGE (Imager for Magnetopause-to-Aurora Global Exploration)[3]	1000 km x 7 R_e polar	Magnetospheric science mission Launch: February 2000
Cluster II[4]	4 R_e x 19.6 R_e	Four spacecraft flying in formation Launch: middle 2000
IMEX (Inner Magnetosphere Explorer)[5]	350 x 35,800 km	Magnetospheric science mission Launch: June 2001
ST5 (Space Technology 5)[6]	A: 500 x 35,700 km B: 3500 x 35,700 km C: 12,756x57,402 km	Validation of formation flying technologies (New Millennium Program)
AMM (Auroral Multiscale Midex Mission)[7]	600 x 7000 km polar	Four spacecraft flying in formation Launch: June 2002
Auroral Lite[8]	1000 x 8000 km polar	Launch:2004 (earliest)
Magnetospheric Multiscale[9]	1200 x 70,160 km 1200 x 185,000 km 7 R_e x 109 R_e 11 R_e x 49 R_e	Four mission phases Four spacecraft flying in formation Launch:ca. 2005-2007
Magnetospheric Constellation[10]	3 R_e perigee 12-42 R_e apogee	Up to 100 satellites, flying in formation Launch: ca. 2007

GPS has been used extensively for satellites in low Earth orbit (LEO), and a few commercial receivers exist that can provide reliable and efficient onboard navigation solutions. In their current form, these receivers are not directly applicable to HEO and GEO missions because of important differences in the vehicle dynamics, signal levels, and geometrical coverage. However, previous flight experiments have provided proof of concept results by demonstrating high altitude tracking of both the GPS main lobe and side lobe signals. The TEAMSAT/YES mission, managed by ESTAC in the Netherlands, demonstrated the first acquisition of GPS signals above the constellation in 1997[11]. The EQUATOR-S mission, which carried a Motorola Viceroy 12-channel GPS receiver as a technology experiment, demonstrated tracking of GPS satellites at altitudes of up to 34,000

km[12]. The Falcon Gold experiment, conducted by the Air Force Academy, studied the GPS signals from a highly elliptical (geostationary transfer) orbit by taking a "snap shot" of the GPS signal spectrum, with the normal receiver processing functions performed on the ground in post-process[13]. In addition, a number of studies have been conducted to evaluate the potential application of GPS to other HEO and GEO missions[14,15,16].

Early experiments using heritage GPS receivers have not demonstrated a real time autonomous navigation capability due to limitations in the basic algorithms guiding signal acquisition and tracking. This paper presents a GPS receiver architecture, based on the GSFC PiVoT receiver[17], which will provide an autonomous navigation capability for HEO applications. To achieve this goal, the criteria for selecting satellites and the search methods to find the Doppler frequency and code offset during the signal acquisition process must be changed. Additionally, the tracking loops must be modified to enhance the receiver's ability to track the weaker signals encountered in these orbits. The expected increase in navigation accuracy corresponding to modest reductions in the tracking threshold is evaluated. It is shown that consideration of tracking loop design in concert with a properly tuned navigation filter can lead to a practical GPS based orbital navigation system for HEO applications.

In addition to the PiVoT, several other new GPS receivers are promising candidates for the HEO/GEO environment because of their flexibility and open architecture, namely the Applied Physics Laboratory GNS receiver,[18] and the Surrey Satellite Technology Limited SGR receiver[19]. Another effort entitled GPS on a Chip (GOAC), is a collaboration involving the Jet Propulsion Lab, the Goddard Space Flight Center, and Stanford University. The goal of GOAC is to produce a low cost modular design that can be configured efficiently for a wide range of unique space applications, eventually evolving the design into a credit card sized package[20].

SPACECRAFT NAVIGATION USING GPS: LEO VERSUS HEO/GEO

The most obvious difference between HEO and LEO operations is the sparse nature of GPS signals at high altitudes. There are rarely four or more satellites visible simultaneously, the condition required for a GPS receiver to produce a point solution for position and time. Furthermore, the available signals are generally very weak and originate from only a small region of the sky. This stresses both the ability of the receiver to acquire and track the signals and the quality of the navigation solution obtained.

From a low Earth orbit, signals from ten or more GPS satellites are typically visible, received with uniform power levels and geometric distribution above the local horizon. Except for the Doppler frequency and the rapid rise and set times of new satellites, this is not unlike the visibility presented to terrestrial GPS users. Our simulations have shown that above altitudes of approximately 3500 km, corresponding to the 21.3 degree main beam limit for the transmitted L1 signal, these conditions become much less favorable. As the altitude increases, received signal power typically decreases because 1) the transmitted power of some signals is reduced due to the attenuation pattern of the transmitting GPS satellite and 2) the ranges to many of the visible GPS satellites increase. As a result, the received power levels of signals from many of the GPS satellites *physically* in view are below the tracking threshold of the receiver. For medium altitudes, higher than 3500 km but still below the 20,000 km altitude of the GPS constellation, the total number of visible signals drops off sharply, but these signals can originate from any part of the sky. At the geostationary altitude and above, the visible GPS signals radiate from a narrow cone centered in the direction of the Earth, and GPS signal outages lasting several hours are not uncommon.

Several factors further complicate high altitude GPS operations. Occasionally, a single, powerful signal from a GPS satellite at "close" range will jam all of the other signals being tracked by the receiver, causing loss of lock and a data outage. Through perigee passage of a highly eccentric orbit, the relative line-of-sight velocities (Doppler) will be higher than for any other GPS application, at times greater than +/-10 km/s. Some missions may employ pointing strategies that preclude designers from mounting GPS antennas in the most favorable orientations for receiving GPS signals, further reducing signal visibility. Finally, the radiation environment for HEO spacecraft can be orders of magnitude more severe than in LEO. The 350 by 35,800 km orbit of the IMEX spacecraft is a particularly severe example; the total radiation dose is close to 200 krads/year assuming an aluminum absorber box thickness of 3 mm[5].

HEO/GEO RECEIVER REQUIREMENTS

In order to provide acceptable performance in the presence of the wide range of conditions discussed above, some significant changes must be considered for existing GPS receiver architectures. The following requirements have been identified for a receiver designed for operation in HEO/GEO orbits.

- Radiation tolerance: Through the selection of radiation hardened components, box level shielding, and upset tolerant software, the receiver must survive the extremely severe radiation environment in high altitude orbits. Fully space qualified technology can be too expensive for many small spacecraft, however

at the same time, reliability on-orbit is extremely important[19].

- Stable clock: The importance of an accurate and stable receiver clock is amplified by the requirement to propagate a navigation solution for long periods of time when four satellites are not available simultaneously to produce a three-dimensional position and clock bias solution.
- Robust navigation filter and clock model: A capable and robust navigation filter and clock model is required to enable the receiver to generate solutions when fewer than four satellites are visible simultaneously and to propagate a solution through GPS signal outages. The filter must support rapid re-initialization for missions that require frequent power cycling of the receiver to conserve power.
- Satellite selection and signal acquisition: Criteria other than traditional dilution of precision (DOP) or highest elevation must be used to select and assign satellites to receiver channels for tracking. An estimate of received signal to noise ratio (C/No) should be one of the most important selection criteria. The signal acquisition algorithms may require mission specific customizations and must be robust enough to handle the varying conditions (Doppler, C/No, etc.) experienced over each orbit. Furthermore, the search pattern used to vary code delay and Doppler frequency to look for new satellites must take into account the expected range of Doppler frequencies encountered in these orbits. One potential way to speed up this search is to assign multiple correlator channels to one satellite at different Doppler frequencies.
- Multiple channels: The changing geometric distribution of signals in the sky throughout an orbit requires multiple antennas and antenna orientations to provide the best coverage. The receiver should allow dynamic assignment of correlator channels to antennas to make the best use of the resources in the receiver as conditions change over the course of the mission.
- High gain antennas: Certain nadir pointing spacecraft can utilize high gain receiving antennas to improve signal visibility at high altitudes.
- Weak signal tracking: Specific strategies can be employed to increase the number of GPS signals visible under certain conditions by better enabling the receiver to track weak GPS signals and to take advantage of available side lobe signals. These strategies are explored further below.
- Resistance to jamming: Receiver tracking loops must be resistant to jamming from other GPS space vehicles in close proximity (near-far problem).

PIVOT GPS RECEIVER

The PiVoT receiver has been developed by the GSFC Guidance, Navigation and Control Center to provide a low cost GPS navigation system for NASA's Small Explorer (SMEX) and Spartan series of spacecraft, as well as other LEO orbit and attitude determination applications. PiVoT is based upon the MITEL 2010/2021 chipset and utilizes an open architecture design using an industry standard bus. This allows the use of different processors, as well as possible expansion of the number of RF/Correlator boards. At present, the design of each RF/correlator board calls for 24 correlator channels fed by 4 radio frequency (RF) inputs. The baseline predetection integration time in the 2021 correlator is 1 ms. The PiVoT clock is a high quality temperature-controlled crystal oscillator with a specified root Allan variance < 0.4E-10 for 1 second.

The GPS Enhanced Orbit Determination (GEODE) software is incorporated as a real-time navigation filter in the PiVoT receiver. Initially developed for LEO applications, GEODE consists of an extended Kalman filter, a high fidelity model of the orbital dynamics, and fault detection capabilities . An accuracy of 10 meters position and 0.01 meters/second velocity (1σ)

odular software supports customization of algorithms guiding satellite selection, acquisition, and tracking to optimize the performance for HEO/GEO missions. GEODE filter running in real time enables the operation of the receiver in very sparse signal visibility conditions. Additionally, a new version of the GEODE flight software is being developed with the capability of estimating relative position states between multiple spacecraft flying in formation, a requirement of several of the missions listed in Table 1.

RECEIVER TRACKING THRESHOLDS AND WEAK SIGNAL TRACKING

The tracking threshold has an important impact on GPS receiver performance in HEO applications due to the weaker signals associated with these orbits. Previous analytical studies of GPS visibility in HEOs indicate a significant number of GPS observations present at signal levels just below the tracking threshold of current receivers. It will be shown that even modest improvements in this threshold of only 5 to 7 dB can

translate into better GPS visibility and navigation solution accuracy.

The tracking threshold of an unaided delay lock loop (DLL) is a function of the code loop noise bandwidth, the predetection integration time, and the correlator spacing. The degree to which these three parameters can be changed is limited by a tradeoff against the filter response to dynamic stress. A DLL with an nth order open loop filter will generate a steady state dynamic stress error for the nth derivative of the line of sight path length. For example a second order filter will produce a steady state error in response to acceleration.

A rule of thumb used to predict the tracking threshold is that the DLL will track signals until the 3σ value of the code phase jitter due to all sources exceeds the correlator spacing. The primary contributors to this error are the thermal noise and dynamic stress error, in which dynamic stress enters as a 3σ effect[22]. This model was used to compute the dependence of the tracking threshold on predetection integration time. Figure 1 provides the results for a number of filter bandwidths, assuming no dynamic stress. Similarly, Figure 2 shows the dependence of the C/N_0 threshold on filter bandwidth, for a number of integration times. As these plots indicate, reducing filter noise bandwidth will reduce the C/N_0 threshold. Increasing integration time will also reduce this threshold, with lower effect. Reducing the correlator spacing will result in a lower acquisition threshold as well.

The cost to the optimization of a DLL design through the variation of bandwidth and correlator spacing is the sensitivity to dynamic stress. A narrow filter bandwidth or correlator spacing will result in a filter with a lower tolerance for dynamic stress. The limit to increasing the integration time is set by the 50 Hz data message modulated on the GPS signal. The 20 ms duration of each data bit is the longest time that the correlation can be integrated without integrating across a data bit transition. This limit is indicated by the dashed vertical line on Figure 1. For a filter with 2 Hz bandwidth, Figure 1 indicates an approximate 4 dB reduction in acquisition threshold could be obtained by increasing the integration time to this maximum value. Figure 2 shows that an approximate 2 dB reduction could be achieved by reducing the bandwidth by half for a 1 ms integration time.

It should be noted that the only true measure of tracking threshold performance of a receiver is through experimental tests or Monte Carlo simulations under combined dynamic and signal-to-noise ratio conditions[22]. Furthermore, the rules of thumb tend to predict a more optimistic tracking threshold than is typically achieved in actual receiver implementations due to other power losses associated with A/D conversion and down conversion to intermediate frequency (IF) in the receiver. They do, however, provide an indication of the possible reduction in code tracking loop threshold achievable through design of a stand alone loop given the functional dependence shown in Figures 1 and 2 and limited by the dynamic stress caused by the GPS satellite and receiver motion.

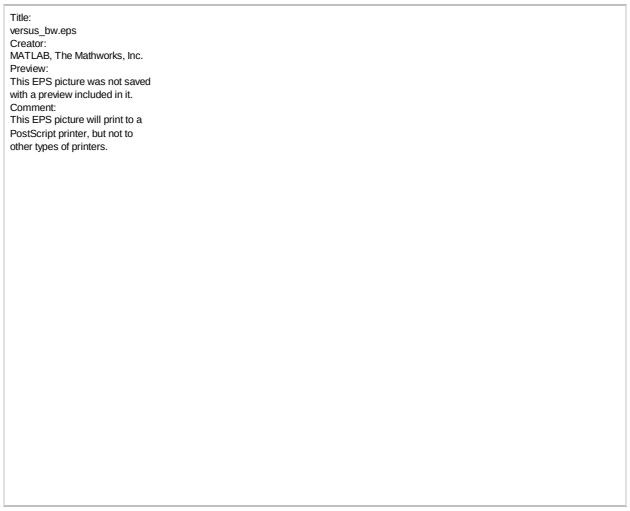

Figure 1: Variation in tracking threshold for various filter bandwidth values.

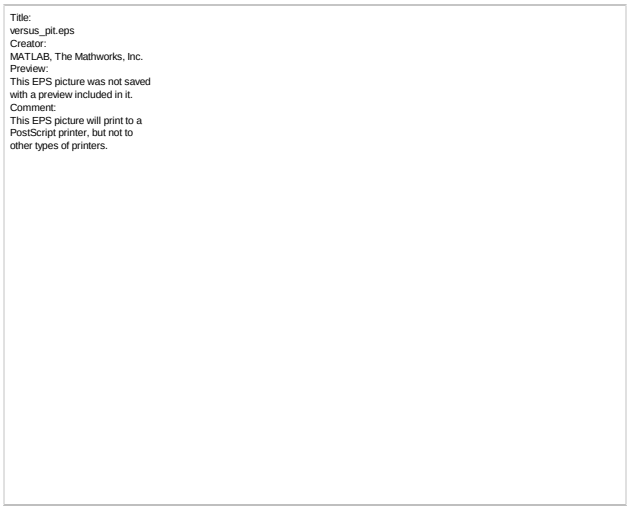

Figure 2: Variation in tracking threshold for various predetection integration times.

In order to reduce the acquisition threshold further, the loop architecture must be modified to incorporate additional information. Several techniques have been developed for other GPS applications and have appeared in the literature that could be applied to varying degrees to the weak signal tracking problem in HEOs. A few potential architectures are described below.

* Date wipeoff: If all or part of the 50 Hz broadcast navigation message is available from an outside source, either from another satellite or stored in the receiver from an earlier time in which a given satellite was tracked, then this data stream can be replayed and used to properly correct for the sign changes in the correlation[22]. This

would allow predetection integration times exceeding 20 ms, however it obviously requires a source of this data. If the desired satellite has not been tracked recently, portions of the data message could be constructed from the data broadcast by other satellites in the constellation. Each 30 second block of data contains ephemeris information unique to each satellite and almanac data and other parameters common to all of the GPS SVs. It is possible to reconstruct the known portions of the message to perform data wipeoff during portions of the 12.5 minute epoch of the full navigation message.

* Loop aiding: The effect of dynamic stress on the tracking loop can be significantly reduced if an estimate of the vehicle velocity and acceleration is present to aid the tracking loop. Landry et al.[23] studied the use of internal GPS velocity aiding from a Kalman filter to improve acquisition time and tracking performance. Unlike aeronautical applications, the dynamics of orbital motion are very well known. That fact makes this technique very promising for reducing the tracking threshold in HEO applications. Furthermore, a Kalman filter with a good dynamic model can be used to propagate the orbit forward using measurements of only one (strong signal level) satellite. For some period of time, the dynamic model alone should be accurate enough to aid the reacquisition of a weak satellite, even at times in which no other satellites are visible. Analysis of this problem will require simulation of the coupled filter-tracking loop system. The tracking loop dynamic stress will be determined by the estimation errors of the navigation filter.

* Vector Delay Lock Loop (VDLL): The idea of coupling the navigation solution and the tracking loops can be extended even further. In contrast to conventional receiver architectures in which the tracking loop is independent from the navigation filter, the VDLL estimates the state directly from the raw GPS data stream. In this manner, the signal to noise ratio of the individual satellite measurements could all be below the acquisition threshold of the receiver as long at the total received power exceeds this threshold[24]. This will therefore make the optimal use of signals from all visible satellites using the fact that the individual received signals are not independent.

* Other hardware architectures: GPS receivers which take a sample of the down converted signal (JPL microGPS[25], Navsys TIDGET[13], etc.) are advantageous for missions not requiring real-time onboard solutions. These systems move the receiver processing functions (correlation, signal detection, data demodulation, etc.) from the receiver to a separate ground based computer to be performed in post-process. One advantage is that the receiver is only powered on for a fraction of each orbit, and therefore can be used on very power-limited missions. Additionally, post-processing enables the use of techniques that would not be possible in real-time on orbit. Another application of a "distributed system" concept to the problem of weak signal detection was recently disclosed in a patent by Moeglein and Krasner[26]. This system, designed for terrestrial applications, obtains the visible PRNs and Doppler from a reference source, and then performs an FFT on a long segment of sampled data. This allows a very long effective integration time, and can thus generate a point solution (for a stationary receiver) from very weak signals, with as much as 25 dB attenuation.

The baseline tracking threshold assumed in this paper for a conventional, unmodified receiver was arrived at through an experimental test of the tracking performance of the Mitel hardware using a static receiver tracking GPS satellites from a rooftop antenna. A variable signal attenuator was inserted between a passive antenna and low noise amplifier. The threshold was measured experimentally to be 35 dB-Hz for acquisition and 34 dB-Hz for tracking. This result compares favorably with the assumed tracking threshold for other GPS receivers (37 dB-Hz and 38 dB-Hz) appearing in the literature[14,15]. To compare the GPS visibility and navigation solution accuracy results for modest improvements in the tracking threshold, three receiver thresholds were simulated: 35 dB-Hz (nominal), 30 dB-Hz (5 dB improvement), and 28 dB-Hz (7 dB improvement).

To evaluate the range of requirements for GPS navigation of HEO missions, we have simulated the GPS signal visibility and navigation performance for several representative HEO missions as a function of receiver tracking threshold. Table 2 provides the parameters for the four HEO mission scenarios examined in this paper. These scenarios are based on three HEO spacecraft missions that are currently proposed or in development and the actual orbit, pointing constraints, and other parameters for these missions have been used. Figure 3 shows a comparison of the shapes of the three orbits in relation to the geostationary altitude and the altitude of the GPS constellation.

The IMEX satellite, scheduled for a June 2001 launch, will measure the populations of energetic particles and related magnetic and electric fields throughout the Earth's radiation belts. The orbit features a low perigee altitude; thus, near perigee the conditions will be similar to that of a LEO spacecraft. The mission design calls for a spin stabilized spacecraft, with the spin axis oriented parallel to the Earth-Sun vector[5]. On a spinning spacecraft, there are only two possible GPS antenna orientations that provide a constant view of single part of the sky for continuous GPS tracking: parallel and anti-parallel to the spin axis. However, these antenna orientations are not necessarily the most favorable for receiving GPS signals.

Table 2: Simulation Parameters

Parameter	IMEX-1[5]	IMEX-2	AMSAT[1]	ST5-C[6]
Epoch date	02/09/99 04:10:00	10/10/98 05:20:00	06/21/98 00:00:00	06/21/98 00:00:00
Orbital period [hours]	10.5	10.5	16.0	23.5
Perigee altitude [km]	349	349	4000	12756
Apogee altitude [km]	35800	35800	47693	57402
Semimajor Axis [km]	24446.0	24446.0	32235.0	41457.0
Eccentricity	0.7248	0.7248	0.67744	0.53846
Inclination [deg]	26.4	26.4	63.4	28.5
Argument of perigee [deg]	137.0	63.4	220.0	0.0
Right asc. of the asc. node [deg]	358.0	80.0	225.0	90.0
Mean anomaly [deg]	0.0	0.0	0.0	0.0
Spacecraft attitude	Spin axis parallel to Earth-Sun vector	Spin axis parallel to Earth-Sun vector	Three-axis stabilized, Earth pointing	Spin axis perpendicular to ecliptic plane
GPS antenna configuration	Hemispherical antenna with boresight parallel to spin axis Hemispherical antenna with boresight antiparallel to spin axis	Hemispherical antenna with boresight parallel to spin axis Hemispherical antenna with boresight antiparallel to spin axis	Nadir-pointing high gain antenna Zenith-pointing hemispherical antenna	Hemispherical antenna with boresight parallel to spin axis Hemispherical antenna with boresight antiparallel to spin axis

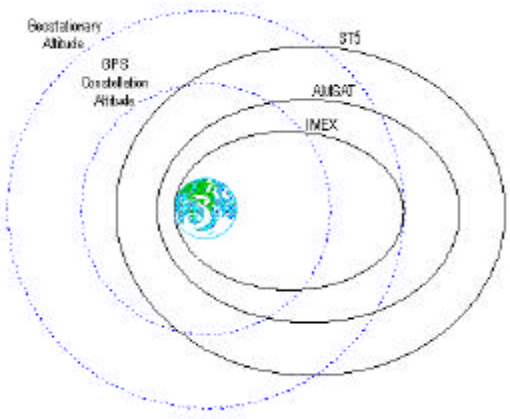

Figure 3: Comparison of the Simulated Orbits.

To illustrate this concept, two IMEX scenarios were examined: one in which the spin axis/GPS antennas are favorably oriented (IMEX-1) and one in which they are not (IMEX-2).

The AMSAT satellite, essentially a communications satellite in a Molynia-type orbit, is three-axis stabilized to maintain one face of the spacecraft in an Earth pointing orientation at all times[1]. At high altitudes, the GPS signals all originate from a narrow cone centered in the nadir direction (toward the Earth). The AMSAT scenario features a high gain GPS antenna on the nadir pointing spacecraft face, to aid in the tracking of the weak GPS signals near apogee, and a typical hemispherical antenna on the zenith-pointing face to improve visibility near perigee. The perigee and apogee altitudes are higher than for the IMEX mission.

Space Technology 5 (ST5) is a component of the New Millennium Program, in which one of the objectives is to validate new technologies applicable to constellations of small satellites[6]. The orbit discussed here is similar to one of the high altitude orbits proposed for the Magnetospheric Constellation Mission (Table 1). This orbit features a very high perigee and apogee, and was selected to provide an example exhibiting very poor GPS visibility throughout the orbit. The spin axis is aligned perpendicular to the ecliptic plane, so the antennas will not necessarily be oriented in the most favorable direction for receiving the GPS signals. Hemispherical antennas, oriented parallel and anti-parallel to the spin axis, are modeled.

SIMULATION PROCEDURE

A simulation was performed to model the GPS visibility and compute simulated GPS pseudorange measurements for the HEO mission scenarios described above. For each scenario, three sets of pseudoranges were generated, corresponding to three different values of the receiver tracking threshold. Using the simulated data, the expected navigation solution accuracy for the AMSAT and ST5 missions was evaluated using GEODE. The following procedure was followed:

1. The truth ephemeris for each host satellite was generated using the Goddard Trajectory Determination System (GTDS) with the high-accuracy force model parameters listed in Table 3. GTDS is the primary orbit determination program used for operational satellite support at GSFC[27].

2. The GPS satellite orbits were generated using the broadcast ephemeris for the simulation epoch.

Table 3. HEO Truth Ephemeris Force Model Parameters

Parameter	Value
Nonspherical Earth gravity model	50x50 Joint Goddard Model (JGM)-3
Solar and lunar ephemerides	Jet Propulsion Laboratory Definitive Ephemeris (DE) 200
Spacecraft area model	Spherical
Solar radiation pressure coefficient	1.4

Table 4: GPS Visibility Simulation Parameters

Parameter	Value
Simulation time span	3 days
Measurement interval	All visible satellites every 60 seconds
GPS SV orbits	Broadcast ephemeris for June 21-23, 1998
GPS SV characteristics	
SA errors	25 meter (1-sigma)
Transmitting antenna pattern	GPS L-Band Antenna Pattern[28], modeled to 90 deg. down from boresite (90 deg. half angle)
Transmitted power	28 dBW in maximum gain direction
User antenna model:	
Hemispherical antenna:	maximum gain: 3.5 dBic horizon mask: 90 deg from boresite
High gain antenna:	maximum gain: 9.2 dBic horizon mask: 56 deg from boresite
GPS receiver characteristics	receiver noise figure: 2.9 dB system noise temperature Earth pointing antenna: 290K Otherwise: 180K 12-channels with GPS SV signals selected based on highest signal-to-noise ratio 35, 30, or 28 dB-Hz receiver acquisition thresholds
Visibility constraints	Earth blockage, with 50 km altitude atmospheric mask transmitting antenna beamwidth and receiving antenna horizon masks received C/N_0 above tracking threshold
Ionospheric delays	Included
Receiver clock bias white noise standard deviation for 60 second rate	0.72 m
Receiver clock drift rate white noise standard deviation	7.5×10^{-5} m/s

3. GPS pseudorange measurements were simulated using the parameters listed in Table 4. A GPS satellite was considered visible and a pseudorange measurement generated for it if the following conditions were satisfied:

- Geometric line of sight (LOS) to the GPS satellite is unobstructed
- Received signal power is above the receiver tracking threshold
- Twelve receiver channels are assumed; when more than 12 GPS SVs are visible, the signals with the highest C/N_0 are selected for tracking

Output parameters include estimates of the number of visible satellites, pseudorange, received C/N_0, Doppler, and other parameters of interest for each antenna defined in a particular scenario.

4. The simulated GPS pseudorange measurements were processed using GEODE to produce navigation solutions for selected scenarios.

Modeling C/N_0 of Received Signals:

The C/N_0 of the GPS signals reaching the host spacecraft is an important factor in determining if a particular GPS SV can be tracked by the receiver. Several authors have provided thorough discussions on the GPS link budget, and the procedure to estimate the received C/N_0 for the GPS signals in HEO applications[14,15]. The assumptions used in this simulation are listed in Table 4 and are discussed briefly here.

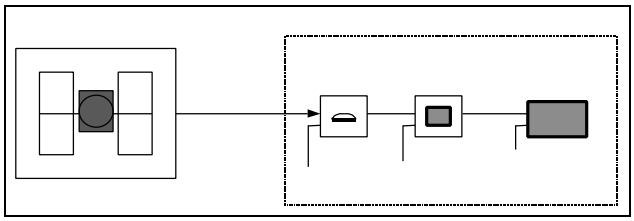

Figure 4: The GPS Signal Transmission Path.

The signal strength at the GPS receiver's location is modeled assuming the GPS signal transmission path illustrated in Figure 4. The isotropic received power (IRP), or GPS signal power at the output of a unity gain RCHP antenna, is

$$IRP = EIRP + A_t + A_d + A_e$$

where $EIRP + A_t$ is the transmitted power along the LOS direction, assuming the standard GPS SV attenuation pattern with effective isotropic radiated power (EIRP) of 28 dBW. A_d is the loss due to propagation of the GPS signals through space, and A_e is the loss due to transmission through the Earth's atmosphere (assumed zero except for very low altitude limb crossing signals). The carrier-to-noise spectral density at the low noise amplifier (LNA) input is computed in terms of the received signal strength by

$$C/N_o = IRP + G_r - 10\log T_{sys} + 228.6 + A_s$$

where G_r is the gain of the receiving antenna in the direction of the GPS satellite, A_s is the system noise figure for the receiver (front end), and T_{sys} is the equivalent system noise temperature[29]. The system noise temperature is bounded by the following two conditions, 1) antenna pointing toward the Earth (T_{sys} = 290K) or 2) antenna pointed elsewhere (T_{sys} = 180K).

The noise figure of the receiver can be computed as follows[30]:

$$A_s = F_1 + (F_2 - 1)/(G_a - L_1) = 2.83 \text{ dB}$$

where

$F_1 = 2.5$ dB noise figure of active antenna LNA
$F_2 = 9$ dB noise figure of GP2010 (RF front end)
$G_a = 26$ dB RF gain of active antenna LNA
$A_c = 2$ dB loss due to RF filtering and cabling after LNA

SIGNAL AVAILABILITY RESULTS

GPS signal visibility results are presented for four scenarios (IMEX-1, IMEX-2, AMSAT, and ST5-C) and three signal tracking thresholds (35, 30, and 28 dB-Hz) in Table 5. In each case, the 35 dB-Hz case represents the performance of the nominal GPS receiver. The specifications for each scenario were provided in Table 2.

Table 5: Summary of GPS Signal Visibility Results

Scenario		Percent of Time One or More Satellites Visible	Percent of Time Four or More Satellites Visible	Antenna Off-Nadir Angle at Apogee
IMEX-1	35	90.0	24.0	5.2 degrees
	30	96.0	37.0	
	28	98.7	59.0	
IMEX-2	35	62.0	21.0	85.1 degrees
	30	82.0	34.0	
	28	91.0	41.0	
ST5-C	35	44.0	6.0	66.6 degrees
	30	71.0	16.0	
	28	78.0	22.0	
AMSAT	35	87.0	14.0	0.0 degrees
	30	98.0	43.0	
	28	99.8	66.0	

IMEX

Two scenarios were examined for the IMEX orbit, to compare the visibility at two different times in the mission. The GPS antennas for the IMEX spacecraft are aligned with the spacecraft spin axis, parallel and anti-parallel to the Earth-Sun vector. The IMEX-1 scenario (Figure 5) is selected to illustrate a favorable orientation of the GPS antennas, in which the spin axis is oriented 5.2 degrees off-nadir. The IMEX-2 scenario (Figure 6), with the spin axis oriented 85.1 degrees off-nadir at apogee, illustrates an unfavorable antenna orientation. Visibility results for two full orbits are presented for each.

Clearly the visibility is best for several hours centered at perigee and degrades as the altitude increases. Also apparent, the visibility near apogee is better for IMEX-1 than for IMEX-2. The difference between these two scenarios is attributed solely to the less favorable antenna orientations for IMEX-2, which results in GPS signals received at low elevation angles and reduced gain relative to the receiving antenna pattern.

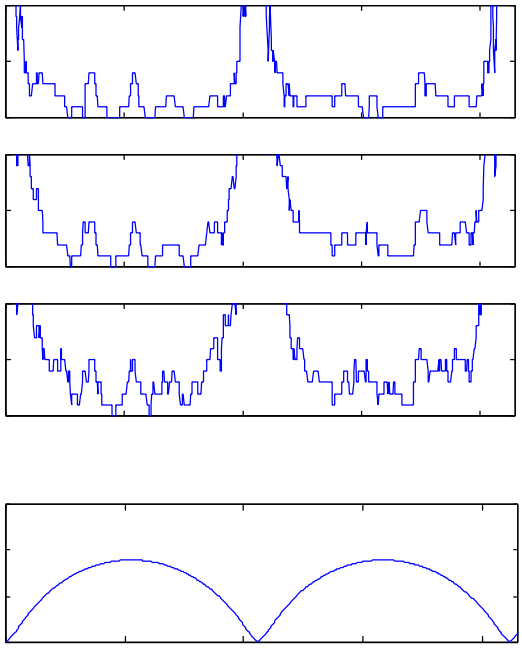

Figure 5: Number of Visible GPS Signals for IMEX-1 Scenario, Favorable Antenna Orientations

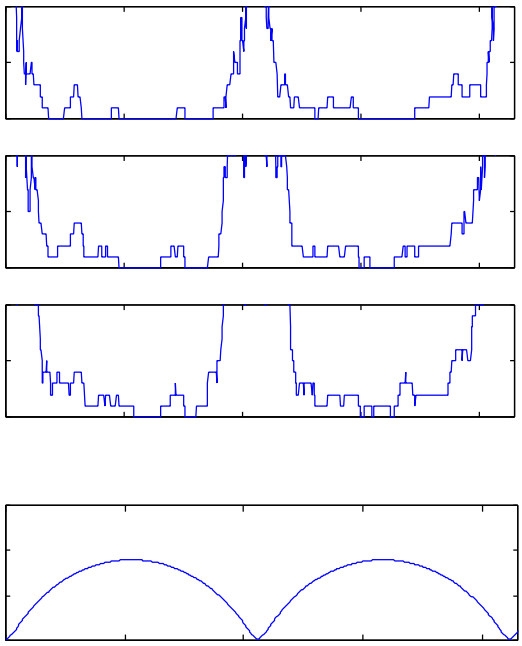

Figure 6: Number of Visible GPS Signals for IMEX-2 Scenario, Unfavorable Antenna Orientations

As summarized in Table 5, for the nominal 35 dB-Hz threshold, four or more satellites are visible simultaneously for better than 20 percent of each orbit. This represents a two hour period centered at perigee when three dimensional positioning is possible. There is at least a single GPS satellite visible 90 percent of the time for the IMEX-1 scenario, compared to only 62 percent of the time for IMEX-2. This large difference is attributed to the long GPS signal outages shown at high altitudes for the IMEX-2 scenario.

Even small improvements in the signal tracking threshold result in noticeable improvements in GPS visibility. For IMEX-1, the percentage of time that four or more satellites are visible simultaneously increases from 24 percent to 59 percent for a 7 dB improvement in the tracking threshold. For IMEX-2, the improvement is only 20 percent.

ST5-C

Results for the ST5-C scenario are provided in Figure 7. For the nominal 35 dB-Hz threshold, there are four or more satellites visible only 6 percent of the time, which corresponds to slightly more than one hour out of each 23 hour orbit. Perhaps even more significant, there are no GPS satellites visible 56 percent of the time. Reducing the tracking threshold by 7 dB results in four or more satellites visible 22 percent of the time, and one or more satellites visible 78 percent of the time (see Table 5). Many of the additional satellites visible for the reduced threshold cases are side lobe radiation from the GPS satellites.

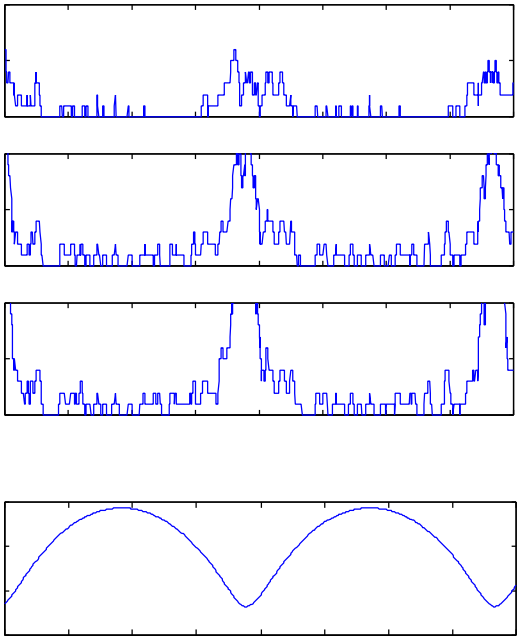

Figure 7: Number of Visible GPS Signals for ST5-C Scenario

While some improvement in visibility is evident near perigee, the very high perigee altitude (over 12,000 km) results in poor GPS visibility throughout the orbit. The most favorably oriented antenna near apogee is off-nadir by approximately 67 degrees, meaning that many of the signals at high altitudes are received at low elevation angles, and reduced gain, with respect to the receiving antenna.

AMSAT

The visibility for the AMSAT orbit is given in Figure 8. For the 35 dB-Hz case, one or more satellites are visible 87 percent of the time, while four or more satellites are visible for 14 percent of the time. As seen in the other cases, these numbers show improvement for 5 and 7 dB reduction in the tracking threshold (Table 5). The AMSAT apogee altitude is between that of IMEX and ST5, however the visibility near apogee is better, or at least more uniform, than for either of those cases. A GPS antenna mounted on the nadir pointing spacecraft face is always ideally oriented for receiving GPS signals at high altitudes. This enables the use of a high gain nadir antenna, which adds almost 6 dB signal gain above that of the hemispherical antennas used in the other scenarios. A hemispherical antenna is still used in the zenith pointing direction.

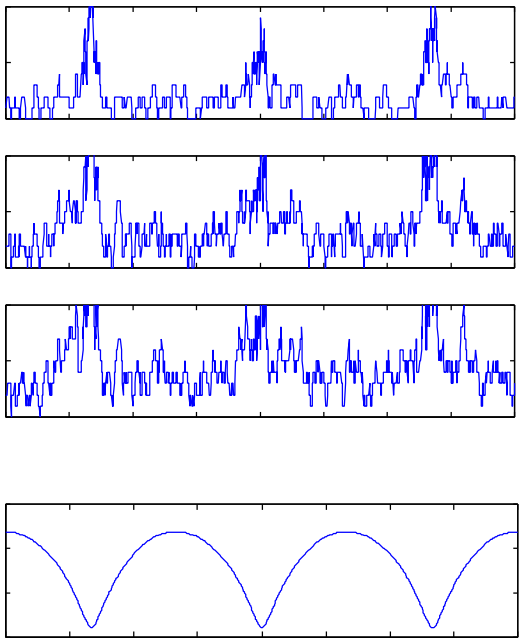

Figure 8: Number of GPS signals visible for AMSAT scenario

At a perigee altitude of 4000 km, the number of visible GPS satellites is significantly reduced compared to the IMEX perigee or to a typical LEO orbit. The 4000 km altitude is just outside of the 21.3 degree main beam limit of the transmitted L1 signal, which coincides with a sharp

drop in the number of visible satellites. Even at perigee, about half of the visible satellites are contributed by the down-looking (Earth pointing) antenna.

Some additional observations were made with respect to the Doppler and C/N_0 levels measured in the simulations. Spacecraft velocities are relatively high in LEO, and the Doppler for visible signals ranges between +/- 8 km/s. In general, as the spacecraft altitude increases, and it's velocity decreases, the range of possible signal Doppler values becomes smaller. For the IMEX scenario, the Doppler range at perigee is actually greater than for LEO (+/- 10 km/s), however for most of the orbit it is much less (+/- 3 km/s near apogee). For the ST5-C orbit, the high perigee altitude results in a maximum Doppler range at perigee of only +/- 5 km/s. In most cases, if the receiver has even a crude knowledge of it's location in orbit, the uncertainty in the frequency dimension of the satellite acquisition process will be significantly reduced compared to that in a LEO.

Examination of the computed C/N_0 of the visible signals revealed several examples of the near-far problem, in which a strong signal from one GPS satellite can jam the ability of the receiver to track other GPS signals. When the C/N_0 estimates were plotted over a three day interval, each scenario showed at least one example of a power spike for a single GPS satellite. Each instance resulted from the GPS receiver passing within close proximity (several thousand km) of a GPS satellite. In the AMSAT and ST5-C scenarios, the jamming satellite power was more than 30 dB higher than the next highest signal. While these spikes never last for more than 5 or 10 minutes, they are certainly high enough to cause the receiver to loose lock on any other satellites being tracked.

NAVIGATION PERFORMANCE RESULTS

The ST5-C and AMSAT GPS observation sets were processed with GEODE to study the expected accuracy of the navigation solutions for these scenarios. Table 6 lists the GEODE processing parameters.

Figure 9 compares the steady-state position and velocity errors for ST5-C. The nominal GPS tracking threshold case (35 dB-Hz) results in total position and velocity RMS accuracy of about 100 m and 6 mm/s. Errors increase up to 200 m and 14 mm/s following apogee and reduce to below 30 m and 7 mm/s near perigee. The increase in position and velocity errors approaching perigee occurs during a period with poorest GPS visibility and increasing velocity. Table 7 summarizes the root-mean-square (RMS) and maximum navigation solution results.

Table 6: GEODE Processing Parameters

Parameter	Value
Nonspherical Earth Gravity model	30x30 Joint Goddard Model (JGM)-2
Solar and lunar ephemeris	Low-precision analytical ephemeris
Initial position error in each component	100 m
Initial velocity error in each component	1 m/s
Initial receiver time bias error	100 m
Initial receiver time bias rate error	0.1 m/s
Estimated state	• User position and velocity • GPS receiver time bias and time bias drift
Initial RIC position variances	$(1 \times 10^{+6}, 1 \times 10^{+6}, 1 \times 10^{+6})$ m^2
Initial RIC velocity variances	$(1, 1, 1)$ m^2/s^2
Initial receiver time bias variance	10000 m^2
Initial receiver time bias rate variance	1 m^2/s^2
Measurement data covariance	150.0 m

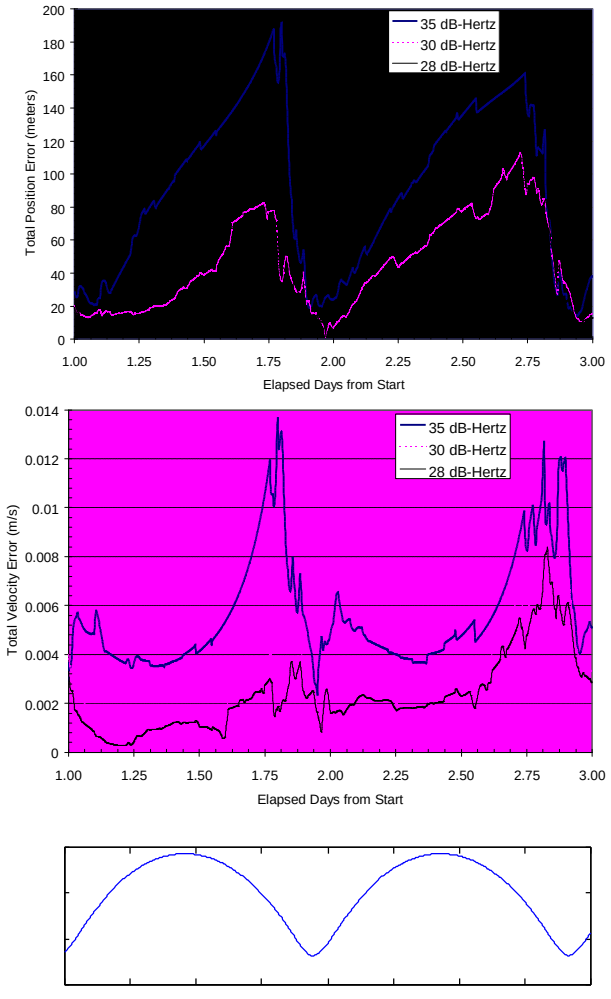

Figure 9: Comparison of Steady-State Position and Velocity Errors for ST5-C

A 5 dB improvement in the tracking threshold reduces the total position and velocity errors by about 50 percent. An additional 2 dB reduction in the tracking threshold further reduces the total position and velocity errors by an additional 10 percent. The accuracy of the estimated clock bias improved from 14 m (0.046 μs) RMS with the 35 dB-Hz threshold to 12 m (0.040 μs) with the 30 dB-Hz and 28 dB-Hz thresholds.

Figure 10 compares the steady-state position and velocity errors for AMSAT. The nominal threshold case (35 dB-Hz) results in total position and velocity RMS accuracy of about 25 m and 3 mm/s, with errors increasing up to 55 m and 10 mm/s following apogee and reducing to below 15 m and 1 mm/s after perigee. The increase in the velocity error approaching perigee is proportional to growth in the satellite velocity from apogee to perigee.

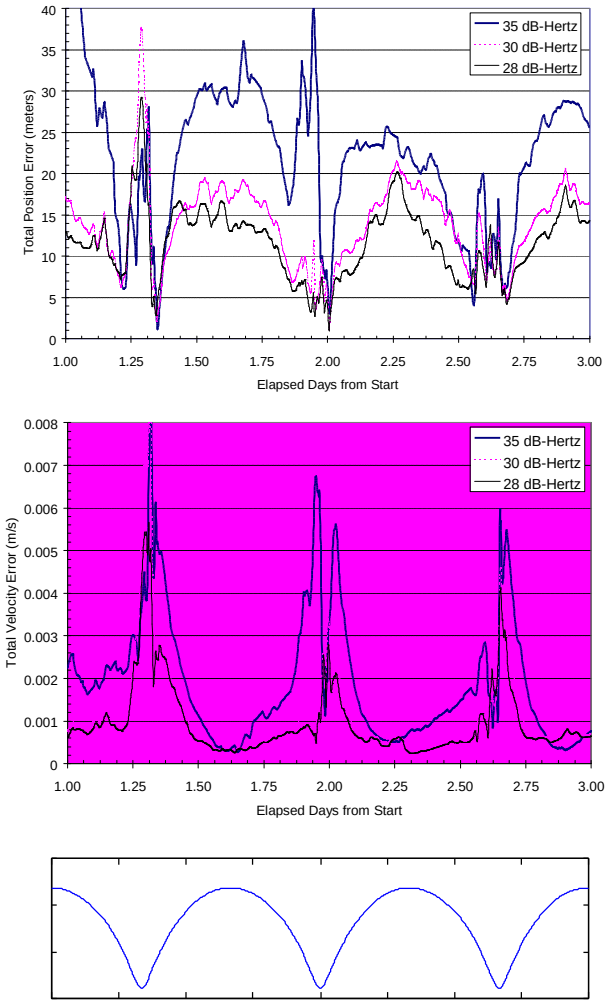

Figure 10: Comparison of Steady-State Position and Velocity Errors for AMSAT

A 5 dB improvement in the tracking threshold reduces the RMS and maximum position and velocity errors by about 30 percent. An additional 2 dB improvement reduces the position and velocity errors by about an additional 20 percent. The accuracy of the estimated clock bias improved from 13 m (0.043 μs) RMS with the 35 dB-Hz threshold to 7 m (0.023 μs) with the 30 dB-Hz threshold and to 6 m (0.020 μs) with the 28 dB-Hz threshold.

Table 7: Summary of Navigation Solution Results

Scenario		Position Error (Meters)		Velocity Error (Millimeters/Second)	
		RMS	Maximum	RMS	Maximum
ST5-C	35	103	192	5.7	13.7
	30	54	113	3.3	8.3
	28	46	96	2.8	8.4
AMSAT	35	24	55	2.4	9.8
	30	15	38	1.7	8.5
	28	12	29	1.3	5.7

In both simulations, the GEODE filter was initialized assuming the initial state vector is obtained from a point solution computed by the GPS receiver, accurate to within 100 m and 1 m/s. A point solution requires simultaneous pseudorange measurements from a minimum of four GPS satellites. Inspection of ST5-C visibility (Figure 7) indicates that point solution computation would rarely be possible using a receiver with a 35 dB-Hertz threshold and would be possible only near perigee with the lower thresholds.

If a point solution is not available, the navigation filter can be initialized using a state vector estimated on the ground, propagated ahead in time, and uplinked to the satellite. This initialization scenario was simulated by applying initial position errors of 0.1, 1.0, and 0.3 kilometers in the radial, in-track, and cross-track directions and initial velocity errors of 1.0, 0.1, and 0.3 meter per second in the radial, in-track, and cross-track directions. The larger initial errors had no significant impact on the steady-state navigation performance for any of the receiver threshold levels.

If neither a point solution nor ground tracking information are available then it is possible to process a long arc of pseudorange data from the satellites that are visible using a batch least-squares estimator. This would provide an autonomous filter initialization process, however the expected accuracy of this method has not been evaluated.

DISCUSSION

The predicted GPS signal visibility and navigation accuracy for some representative HEO mission scenarios were given above. These results provide an indication of

the expected performance of the HEO GPS receiver architecture discussed earlier, considering all of the factors that affect the ability of the receiver to ultimately produce pseudorange measurements in these orbits. The real emphasis for this paper, however, is on the level of improvement that could be gained by signal tracking enhancements rather than the absolute navigation accuracy possible for these orbital scenarios.

The ability of the GPS receiver to produce the above navigation results and the ability to reduce the tracking threshold and improve GPS visibility are interdependent. If the receiver produces steady state navigation solutions accurate to within 200 m and 15 mm/s, this information coupled with knowledge of the orbital dynamics can be used to improve the signal tracking threshold. Before the filter converges, however, errors in the propagated state could be quite large. During this initialization process, only strong GPS signals will be visible for tracking; however, by exploiting the known orbital dynamics, even very crude knowledge of the spacecraft position in the orbit will provide valuable information to aid the signal acquisition process.

In both of the scenarios examined, GEODE required one full orbit to converge to a steady-state solution (16 hours for AMSAT and 23.5 hours for ST5-C). Once converged, GEODE was able to tolerate 4-5 hour signal outages each orbit in the ST5 case and reconverge within 1-2 hours when tracking geometry improved. These results were consistent regardless of whether the filter was initialized with a point solution or a state vector generated on the ground. It is desirable for many low cost spacecraft to power down the GPS receiver during portions of the orbit, especially at times when large data outages exist for hours at a time. It is expected that convergence times can be reduced by optimizing the filter for highly eccentric orbits and by processing accurate GPS Doppler measurements in addition to pseudorange measurements. Initialization methods using Doppler measurements will be implemented to provide the capability for autonomous initialization when measurements from fewer than four GPS satellites are available. The performance of the receiver at initialization will obviously be best when the receiver is passing through perigee (a good GPS visibility region).

The importance of an accurate and stable receiver clock was mentioned briefly earlier. The reason spaceborne GPS systems are able to function well even with sparse data is well known dynamics. In this environment, the limitation to the state prediction process in the filter is the predictability of the oscillator. If oscillator rate variation is kept within dynamic uncertainty of orbit propagation, there will be a benefit from even 1 satellite observation. If the oscillator is poor, one satellite does not provide much information about the orbit because all the information is essentially required to maintain clock information. The high quality temperature-controlled crystal oscillator selected for the PiVoT receiver and modeled in these simulations approaches the best performance possible in a cost constrained design.

CONCLUSIONS

The PiVoT receiver is a good candidate for application to GPS navigation in HEO and GEO orbits. The existing design already meets many of the requirements for HEO GPS operations, and GEODE enables an orbit solution when fewer than four GPS satellites are visible and enables the receiver to coast through long data outages. Furthermore, the modular nature of the hardware and software allows customizations that enable the receiver to take the best advantage of the sparse GPS signals available at high altitudes.

Several weak signal tracking strategies developed for other GPS applications are applicable to varying degrees to the weak signal tracking problem in HEO/GEO orbits. Improvements in the receiver tracking threshold of up to 5 dB are relatively easily achieved through internal velocity aided to narrow the tracking loop bandwidths and increase integration times. Several more involved techniques could be applied to achieve significantly greater reductions in the tracking threshold. Simulation results indicate good navigation solution results for the proposed HEO receiver architecture in several different HEO scenarios. Modest reductions of 5-7 dB in the tracking threshold result in noticeable improvements in navigation solution accuracy; 50-60 percent for the poor visibility ST5-C case, and 30-50 percent for the AMSAT case.

The results suggest that the proposed receiver architecture will enable the use of GPS as an autonomous navigation sensor in HEO and GEO applications, satisfying a requirement for many future flight projects. Future work toward this goal will include implementation and testing of modified tracking loop architectures in a software receiver and on the Linux-based PiVoT development system and further testing using a GPS constellation simulator. Improved tuning for highly eccentric orbits and the processing of accurate GPS Doppler measurements in addition to pseudorange measurements are expected to reduce convergence times of the navigation filter. The receiver discussed in this paper will provide an autonomous, real time navigation capability for HEO missions that does not currently exist today.

ACKNOWLEDGEMENTS

The authors would like to acknowledge Taesul Lee of Computer Sciences Corporation and Russell Carpenter of Goddard Space Flight Center who contributed to the navigation solution analysis.

REFERENCES

[1] R. Zimmerman, P3-D Spacecraft: overview, http://128.54.16.15/amsat/sats/phase3d/, June 99.

[2] J. Neelon, et al., "Orbit Determination for Medium-Altitude Eccentric Orbits Using GPS," AAS/AIAA Space Flight Mechanics Meeting, Breckenridge, CO, Feb. 1999.

[3] E.V. Bell, Imager for Magnetopause-to-Aurora Global Exploration, http://image.gsfc.nasa.gov/, June 1999.

[4] ESA: Cluster II Mission, http://sci.esa.int/missions/cluster/, June 1999.

[5] Personal communication with S. Jones, Laboratory for Atmospheric and Space Physics, University of Colorado at Boulder, Nov. 1998.

[6] Space technology 5 – Technology Announcement, http://nmp.jpl.nasa.gov/st5/st5-announce.html, June 1999.

[7] Auroral Multiscal Midex (AMM) at JHU APL, http://sd-www.jhuapl.edu/AMM/, June 1999.

[8] Personal communication with Dr. Steven A Curtis, Code 695, GSFC, June 14, 1999.

[9] Magnetospheric Multiscale Mission, http://umbra.nascom.nasa.gov/SEC/secr/missions/MMM2.html, June 1999.

[10] Magnetospheric Constellation, http://stprobes.gsfc.nasa.gov/magcon.htm, June 1999.

[11] TEAMSAT Results, April 1998. http://www.estec.esa.nl/teamsat/page_menu_results.html

[12] O. Balbach, et al., "Tracking of GPS Above GPS Satellite Altitude: Results of the GPS Experiment on the HEO Mission EQUATOR-S," *Proceedings of the Institute of Navigation GPS 98 Conference*, Nashville, TN, 1998.

[13] G. Belle et al, "The U.S. Air Force Academy GPS Flight Experiment Using the Navsys TIDGET," *Proceedings of the Institute of Navigation GPS 97 Conference*, Kansas City, MO, 1997.

[14] J. Potti, P. Bernedo, A. Pasetti, "Applicability of GPS-based Orbit Determination Systems to a Wide Range of HEO Missions," *Proceedings of the Institute of Navigation GPS 95 Conference*, Salt Lake City, UT, September, 1995, pp. 589-598.

[15] B. Eissfeller, O. Balbach, U. Rosbach, "GPS Navigation on the HEO Satellite Mission EQUATOR-S, Results of the Feasibility Study," *Proceedings of the Institute of Navigation GPS 96 Conference*, Kansas City, MO, 1996, pp. 1331-1340.

[16] P. Ferrage, et al., "GPS Techniques for Navigation of Geostationary Satellites," *Proceedings of the Institute of Navigation GPS 95 Conference*, Salt Lake City, UT, September, 1995, pp. 257-268.

[17] Bauer, F., Hartman, K., and Lightsey, E. G., "Spaceborne GPS Current Status and Future Visions," *Proceedings of the Institute of Navigation GPS 98 Conference*, Nashville, TN, September 1998, pp. 1493-1508.

[18] W. Devereux et al., "The TIMED GPS Navigation System (GNS)," 49th International Astronautical Congress, Sept. 28-Oct. 2, 1998.

[19] M.J. Unwin et al., "The Use of Commercial Technology for Spaceborne GPS Receiver Design," *Proceedings of the Institute of Navigation GPS 98 Conference*, September, 1998, pp. 1983-1989.

[20] Meehan, T., et al., "GPS on a Chip – An Advanced GPS Receiver for Spacecraft," *Proceedings of the Institute of Navigation GPS 98 Conference*, Nashville, TN, 1998, pp. 1509-1517.

[21] Goddard Space Flight Center, Flight Dynamics Division, CSC-96-932-07R0UD0, *Global Positioning System (GPS) Enhanced Orbit Determination (GEODE) System Description and User's Guide*, Version 4, A. Long et al., prepared by Computer Sciences Corporation, February 1999.

[22] P. Ward, "Satellite Signal Acquisition and Tracking," Ch. 5 in E. Kaplan (editor), *Understanding GPS: Principles and Applications*, Artech House Publishers, 1996.

[23] Landry, R., Lestarquit, L., Issler, J-L., "Studies on Acquisition and Tracking Threshold's Reduction for GPS Spaceborne and Aeronautical Receivers," *Proceedings of the Institute of Navigation GPS 98 Conference*, Nashville, TN, 1998, pp. 619-624.

[24] J.J. Spilker, "Fundamentals of Signal Tracking Theory," chapter 7 in B. Parkinson et al. (editors), *Global Positioning System: Theory and Applications*, Vol. 1, Progress in Astronautics and Aeronautics, 1997.

[25] S-C Wu, et al., "MicroGPS for Orbit Determination of Earth Satellites," *Proceedings of the ION National Technical Meeting*, Santa Monica, CA, Jan 22-24, 1996.

[26] M. Moeglein, N. Krasner, " An Introduction to SnapTrack Server-Aided GPS Technology," *Proceedings of the Institute of Navigation GPS 98 Conference*, Nashville, TN, 1998.

[27] *Goddard Trajectory Determination System (GTDS) Mathematical Theory*, NASA Goddard Space Flight Center, June 1989.

[28] F. Czopek, "Description and Performance of the GPS Block I and II L-Band Antenna and Link Budget," *Proceedings of the Institute of Navigation GPS 93 Conference*, pp. 37-43.

[29] P. Ward, "Effects of RF Interference on GPS Satellite Signal Receiver Tracking," E. Kaplan (editor), *Understanding GPS: Principles and Applications*, Artech House Publishers, 1996.

[30] GEC Plessey Semiconductors, *GPS Builder-2 Designer's Guide*, April, 7, 1995.